RPC Technical Report No. 1276-102-G-AR

Final Report

Diffractive Optics Technology and the NASA Geostationary Earth Observatory (GEO)

31July 1992

G. Michael Morris, Robert L. Michaels, and Dean Faklis

Rochester Photonics Corporation
80 O'Connor Road
Fairport, NY 14450

Phone: (716) 377-7990
Fax: (716) 377-7913

Under Contract H-13026D, NASA Marshall Space Flight Center, 35812

Abstract

Diffractive (or binary) optics offers unique capabilities for the development of large-aperture, high-performance, light-weight optical systems. The Geostationary Earth Observatory (GEO) will consist of a variety of instruments to monitor the environmental conditions of the earth and its atmosphere. The aim of this investigation is to analyze the design of the GEO instruments that are being proposed and identify the areas in which diffractive (or binary) optics technology can make a significant impact in GEO sensor design. Several potential applications where diffractive optics may indeed serve as a key technology for improving the performance and reducing the weight and cost of the GEO sensors have been identified. Applications include: the use of diffractive/refractive hybrid lenses for aft-optic imagers, diffractive telescopes for narrowband imaging, sub-wavelength structured surfaces for anti-reflection and polarization control, and aberration compensation for reflective imaging systems and grating spectrometers.

Diffractive Optics Technology and the NASA Geostationary Earth Observatory (GEO)

Table of Contents

List of Figures

List of Tables

Diffractive Optics Technology and the NASA Geostationary Earth Observatory (GEO)

Rochester Photonics Corporation
80 O'Connor Road
Fairport, New York 14450

Phone: (716) 377-7990
Fax: (716) 377-7913

1.0 Introduction

In both government and commercial systems, many new and interesting uses are being found for diffractive (or binary) optics technology. Diffractive optics provide the potential to reduce significantly the size, weight, and cost of a variety of optical instruments that currently utilize refractive and/or reflective optical components.

The Geostationary Earth Observatory (GEO) will consist of a variety of instruments to monitor the environmental conditions of the earth and its atmosphere. The aim of this investigation is to analyze the design of the GEO instruments that are being proposed and identify the areas where diffractive optics technology can make an impact in GEO sensor design.

In Section 2 a brief description of the fundamental principles of diffractive optics is presented, including basic design principles of diffractive lenses for laser (or narrowband) systems, broadband optical systems, and the use of sub-wavelength structured (SWS) surfaces to reduce surface reflections and for polarization control (space-variant polarizers and wave plates). A list of the documents that were reviewed in this study is contained in Section 3; these documents describe the current design for the various GEO instruments/sensors. In Section 4, we identify potential application areas where diffractive optics may indeed serve as a key technology for improving the performance and stability, and reducing the weight and cost of the GEO sensors. In Section 5, some preliminary optical designs for subsystems employing diffractive lenses are given. Our conclusions and recommendations for further research and development are contained in Section 6.

2.0 Principles of Diffractive Optical Systems

2.1 Fundamental Properties of Diffractive Lenses

Diffractive lenses can significantly reduce the size, weight, and cost of a variety of optical systems, which currently utilize refractive and/or reflective optical components. There have been several recent conferences that address design, fabrication and applications of systems that contain diffractive optics. One can get a good overview of the recent developments in the field by reviewing the proceedings of these conferences [1].

Recent advances in fabrication and replication procedures have made the production of high efficiency, surface-relief (blazed) diffractive lenses practical. Fabrication methods for surface-relief diffractive optics include: photolithography [2], single-point, laser-writer systems [3], and diamond turning [4].

In this section, our objective is to review some of the fundamental properties of surface-relief diffractive lenses, and to illustrate how one can utilize diffractive lenses in the design of both narrowband and broadband optical systems.

A typical surface-relief diffractive lens consists of concentric annular zones [see Fig. 1]. It is useful sometimes to think of a diffractive lens as a "Modulo 2π" lens, i.e., at any given point along the lens all the multiple 2π phase changes have been removed. The radius of the m-th zone boundary, r_m, is determined by the following relation: $\phi(r_m) = 2\pi m$, where $\phi(r)$ is the desired phase profile for the lens; these are called full-period zones. In general, the phase function associated with a symmetric lens is given by $\phi(r) = Ar^2 + Gr^4 + Hr^6 + \ldots$, where $A = \pi/(\lambda_0 F)$, G and H are associated with aspheric coefficients of the emerging wavefront, λ_0 is the design (or center) wavelength, and F is the principal focal length of the lens when the incident wavelength $\lambda = \lambda_0$.

To construct the appropriate surface-relief profile from a spherical refractive lens one starts at the center of the lens, moving radially out from the center. For most cases of practical interest, the surface of the lens is traced until the optical phase difference reaches a value of 2π (equivalently, the optical path difference equals one wave). At that point, the surface-relief structure jumps abruptly back to the center height $h_{max} = \lambda_0/(n(\lambda_0) - 1)$, where $n(\lambda_0)$ is the index of refraction of the lens material at wavelength λ_0. Continue tracing along the surface of the refractive lens until the optical phase difference again reaches a value of 2π, jump back to a height h_{max}, and continue this process until the edge of the refractive lens is reached. The construction process gives rise to a blazed zone-plate-type structure that consists of a series of zones that represents the required phase transformation. While the resulting diffractive lens provides essentially the same phase transformation as the associated refractive lens, it has a number of additional properties.

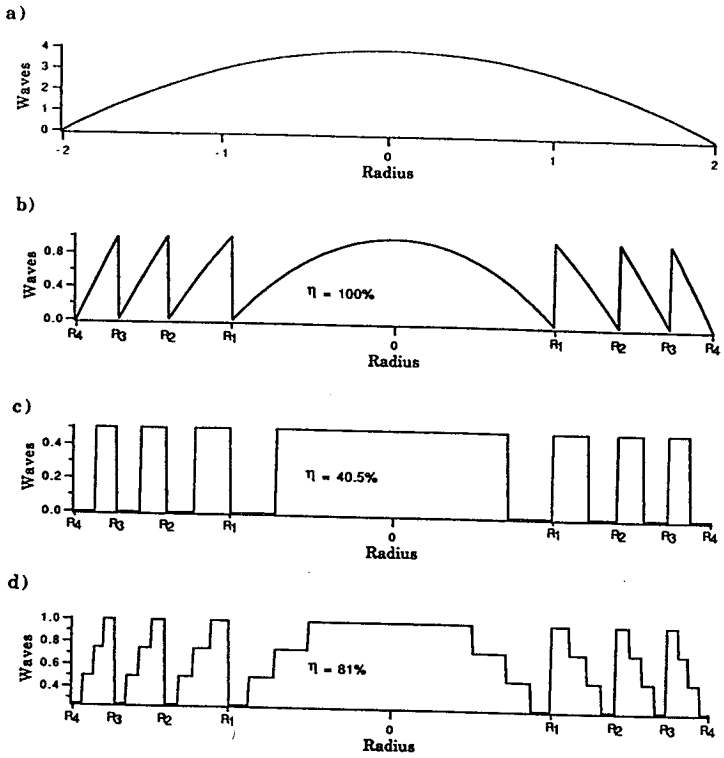

Fig. 1 Diffractive lens construction. (a) conventional refractive lens, (b) diffractive lens with continuous quadratic blaze profile, (c) phase-reversal (or Wood) lens, (d) four-level approximation to quadratic blaze profile.

The spacing of the various zones in a diffractive lens determines the set of possible foci (i.e. the set of possible diffraction orders) and shapes the emerging wavefront. The blaze profile within each zone determines how the incident light is to be distributed among the various foci. In most applications, one tries to maximize the amount of light that goes into a given diffraction order (typically the first diffraction order). As illustrated in Fig. 1(b), with a quadratic blaze profile and using the scalar approximation, one can theoretically direct all of incident light at design wavelength λ_0 into the primary focus, i.e., the diffraction efficiency η is said to be 100%. As is well known, a phase-reversal (or Wood) lens, Fig. 1(c), directs 40.5% of the incident light into the +1 diffraction order and 40.5% into the -1 diffraction order. A four-step approximation to the quadratic phase profile, Fig. 1(d), yields a diffraction efficiency $\eta = 81\%$ in the first diffraction order.

Note that while the schematic drawings may appear similar, a diffractive lens is *not* a Fresnel lens -- the operating principles of the two lenses are completely different. The operation of a diffractive lens is based on the principles of interference and diffraction. One can attribute high diffraction efficiency to the proper design of the surface that produces an emerging wavefront that arrives at the focal point precisely in phase (constructive

interference). On the other hand, the operation of a Fresnel lens is based strictly on the principles of geometrical (or ray) optics. A Fresnel lens typically consists of concentric annular rings that act like an array of prisms. With a Fresnel lens the focal spot consists of an incoherent sum of the contributions from the various prism rings, and the size of the focal spot is determined by the width of the prism facets. To obtain a small focal spot, one chooses a small facet size. However, if the facet width is too small, diffraction spreading associated with the facet aperture will actually increase the size of the focal spot. Hence with a Fresnel lens, diffraction associated with the width of the prism facets places a fundamental limit on the minimum focal spot size that can be obtained. On the other hand, with a diffractive lens the size of the focal spot is determined by the overall aperture of the entire lens -- not the spacing of the individual zones. Hence, diffractive lenses are well suited for use in precision optical systems where high resolution is required.

As an example of the application of diffractive optics to laser systems, Fig. 2 illustrates the performance that can be achieved using a diffractive singlet F-Θ scan lens [5]. The lens drawn schematically in Fig. 2 (a) was designed to operate with a HeNe laser beam at F/20 with a focal length of 325 mm and a scan angle of $\pm 20^0$. Figure 2(b) shows the geometric rms spot size as a function of scan angle for real rays. Figure 2(c) illustrates the scan error (i.e. a measure of the deviation from the F-Θ condition) as a function of field angle. Note that with the single diffractive lens, the geometric spot size is much smaller than the Airy radius, which is approximately 15 μm. The diffractive scan lens in this example was designed using a calculation of the necessary phase transformation to obtain the correct zone spacing and the modulo 2π operation to obtain the appropriate surface profile.

An extremely important property that must be considered in an optical design employing diffractive lenses is the wavelength dependence of the diffractive element. Like a diffraction grating, a diffractive lens is highly dispersive. The focal length $F(\lambda)$ of a diffractive lens varies inversely with the wavelength of the incident light, i.e., $F(\lambda) = F\lambda_0/\lambda$; hence, red wavelengths focus *closer* to the lens than do blue wavelengths, which is just opposite to that produced by ordinary refractive lenses. Because of the strong wavelength dependence associated with a diffractive lens, one might tend to think their use is limited to monochromatic applications; however, this is not the case.

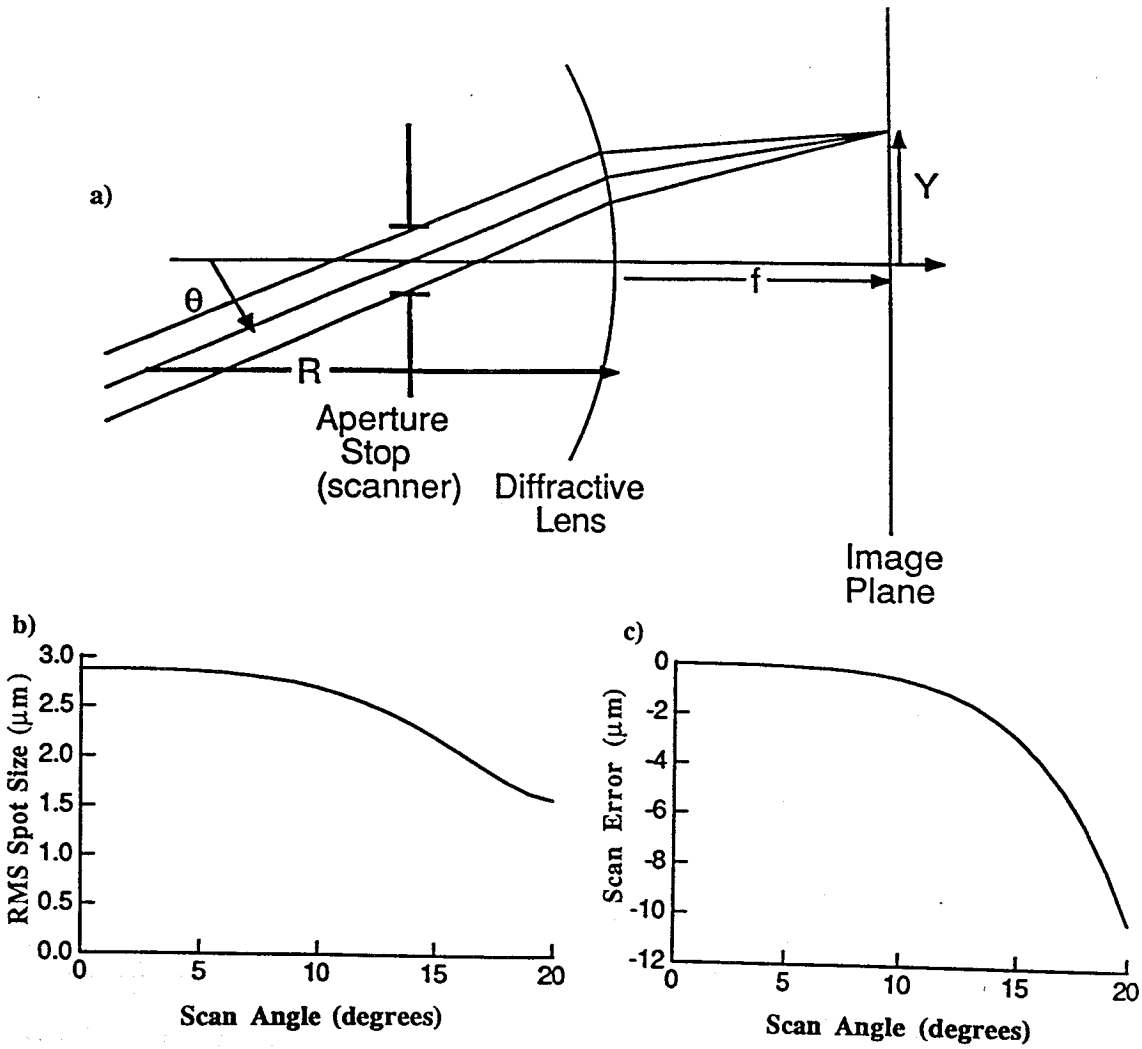

Fig. 2 Diffractive singlet F-Θ laser scan lens. The system layout is illustrated in (a). The geometric spot size for the example described in the text is shown in (b) and the deviation from the F-Θ condition is represented in (c).

When used in combination with refractive elements, diffractive lenses can function effectively in broadband optical systems. For example, an attractive feature of a hybrid diffractive/refractive lens is that a significant reduction in weight can be achieved. Generally, one can reduce the overall lens weight by a factor of two or more. Alignment and mounting of the lens system is greatly simplified, since in most cases the surface-relief diffractive lens is an integral part of the refractive lens surface, and the number of optical elements is minimized. It is also possible to design and build low f-number, diffractive/refractive doublets and triplets that work over large wavelength bandwidths and wide fields of view; this can be quite difficult to do if only refractive lens elements are used.

Design considerations for broadband optical systems consisting of diffractive and refractive lens elements are discussed in Section 2.2.

2.2 Broadband Optical System Design with Diffractive Lenses

Our objective in this section is to illustrate how diffractive lenses can be used in the design of broadband optical systems. We will begin by considering a thin-lens model for a diffractive lens. A first-order layout for an achromatic diffractive/refractive (hybrid) lens will then be described, and factors that affect the performance of hybrid lenses with broadband illumination will be identified.

With commercially available optical design software, there are two basic approaches that one can use to describe a diffractive lens. One approach is to specify (and optimize) a phase polynomial that describes the wavefront to be produced by the lens. The other approach is to model the diffractive lens as a thin, refractive lens with an ultra-high index of refraction [6-8].

The power of a thin-lens, $\Phi_{T.L.}(\lambda)$, can be described by the lens equation:

$$\Phi_{T.L.}(\lambda) = [n(\lambda) - 1]\, c\,, \tag{1}$$

where $n(\lambda)$ is the index of refraction of the lens material at wavelength λ, and c denotes the lens curvature. In References 6 and 7 it is shown that a diffractive lens is equivalent to a thin lens with an infinite index of refraction. Of course, it is impossible to set the index of refraction equal to infinity in a computer. However, it has been found that by taking the model index of refraction, $n_{dif}(\lambda_0)$, of the diffractive lens, at some design (or center) wavelength λ_0, to be approximately equal to 10,000, one can generate results that are virtually indistinguishable from that predicted using either scalar diffraction theory or the phase polynomial description of a diffractive lens [8, 9].

As noted in Section 2.1, the power of a diffractive lens is given by

$$\Phi_{dif}(\lambda) = \frac{\lambda}{F\lambda_0}\,, \tag{2}$$

where F is the principal focal length of the lens when the illumination wavelength λ is equal to λ_0. Equating Eqs. (1) and (2) for the case when $\lambda = \lambda_0$ one finds that

$$c = \frac{1/F}{n_{dif}(\lambda_0) - 1}\,. \tag{3}$$

Using Eqs. (1) - (3), it follows that the model index of refraction $n_{dif}(\lambda)$ for a diffractive lens at wavelength λ (assuming that the lens is using the first diffraction order and is working in air) is

$$n_{dif}(\lambda) = \frac{\lambda}{\lambda_0}[n_{dif}(\lambda_0) - 1] + 1 \quad . \tag{4}$$

If the diffractive lens is on a substrate of curvature c_s, one should take the two surfaces of the model lens to have the following curvatures:

$$c_1 = c_s + \frac{1/F}{2[n_{dif}(\lambda_0) - 1]} \tag{5}$$

and

$$c_2 = c_s - \frac{1/F}{2[n_{dif}(\lambda_0) - 1]} \, . \tag{6}$$

With the thin-lens model, one can use aspheric coefficients to model higher-order terms in the phase polynomial. The thin-lens model also permits easy access to first-order and aberration data.

Let us now consider the first-order design for an achromatic diffractive/refractive (hybrid) lens, as depicted in Fig. 3. In Table I, the relevant parameters for an achromatic doublet are summarized [10]. These parameters include: the lens powers, Φ_{ref} and Φ_{dif}; the Abbe ν-numbers, ν_{ref} and ν_{dif}; and partial dispersions, P_{ref} and P_{dif} for the refractive and diffractive lens elements, respectively. An expression for the secondary spectrum, Δl_{SAC}, for the doublet is also given.

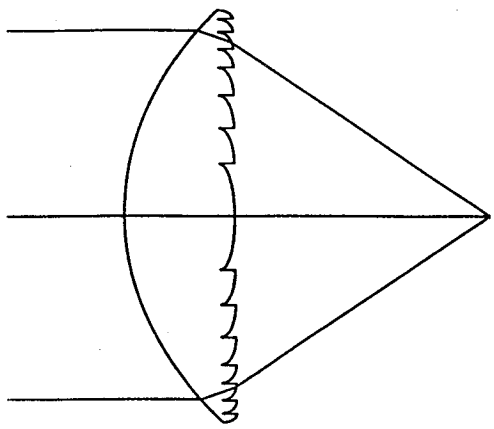

Fig. 3 Configuration for a hybrid, diffractive/refractive, achromatic lens.

In Table II, values for the Abbe ν-number and partial dispersion are given for variety of materials in three different wavelength bands: visible (0.486 - 0.656 μm), mid-infrared (3.0 - 5.0 μm), and far-infrared (8.0 - 12.0 μm). Note that the Abbe ν-number is negative for a diffractive lens, since longer wavelengths focus closer to the lens than do the shorter wavelengths.

In Table III, the calculations for the optical power needed for the various lens elements are summarized. Values of the secondary spectrum for diffractive/refractive doublets are also computed and compared with the values one gets when using conventional refractive materials.

There are several important points to notice in the information contained in Table III. First of all, note that in the diffractive/refractive hybrids, both lens elements have positive optical power. Hence, the power of each lens element is less than F_{total} -- this provides a significant reduction in the amount of required material and weight of the lens. Furthermore, because the Abbe ν-number of the diffractive lens element is so low (i.e., because the diffractive lens is so dispersive), most of the optical power resides in the refractive element. For example, in the Diffractive/BK7 hybrid lens given in Table III, 95% of the optical power resides in the BK7 curvature and only 5% of the total optical power of the doublet resides in the diffractive structure. In this case, the f-number of the diffractive lens element is relatively large, which makes the diffractive element easier to fabricate. Furthermore, alignment and mounting of the lens is greatly simplified, since in most cases the surface-relief diffractive lens can be fabricated as an integral part of the refractive lens surface.

A major goal in the design of an achromatic lens is to minimize the amount of secondary spectrum. As can be seen from the formula for Δl_{SAC} in Table I, a small value for Δl_{SAC} can be obtained by either matching the values for the partial dispersion or by choosing materials that exhibit a large difference in Abbe ν-numbers. Note that in the visible region, the secondary spectrum is considerably larger for the Diffractive/BK7 hybrid lens than for the F2/BK7 lens, whereas for mid- and far-infrared wavelengths the secondary spectrum is quite comparable to that obtained using conventional refractive materials; this makes a diffractive/refractive hybrid lens an attractive candidate for infrared applications, particularly since infrared materials tend to be rather expensive.

There is, however, an additional factor that must be addressed in the first-order design of a diffractive/refractive achromat -- the effects associated with light that is diffracted into other diffraction orders. The diffraction efficiency of a diffractive lens depends on the wavelength of illumination. A reduction in diffraction efficiency in the principal diffraction order implies that there is an increase in the amount of light that

propagates into other diffraction orders, which can contribute to "veiling glare" in the image plane. This will reduce the modulation transfer function (MTF) of the optical system [11,12].

As discussed in Reference 12, a useful figure of merit to describe the effects of non-unity diffraction efficiency on diffractive lens MTF is the "integrated efficiency." In polychromatic applications the integrated efficiency for the wavelength band ranging from λ_{min} to λ_{max} is

$$\eta_{int} = \frac{\int_{\lambda_{min}}^{\lambda_{max}} \eta(\lambda)\, d\lambda}{\lambda_{max} - \lambda_{min}}, \qquad (7)$$

where $\eta(\lambda)$ is the diffraction efficiency for the principal diffraction order at wavelength λ. The integrated efficiency serves as a limiting value and overall scale factor for the MTF. Polychromatic modulation transfer functions for the visible (0.4 - 0.7 μm) and far-infrared (8 - 12 μm) spectral bands are shown in Fig. 4. The reduction in MTF is due primarily to background light associated with the zero-th and second diffraction orders of the lens. However, in many cases, by performing a careful system design, one can greatly reduce the deleterious effects of the background by designing the system so that the majority of the background light is vignetted out of the system. This, of course, does not increase the diffraction efficiency of the lens itself, but it may increase the value of η_{int} measured in the pupil.

There are several advantages afforded by the introduction of surface-relief diffractive elements in many optical systems. These include the correction of wavefront aberrations, reductions in system weight and cost, and the generation of phase transformations that were previously impossible to realize. New fabrication techniques are becoming available to help reduce the cost of tooling for master and prototype elements.

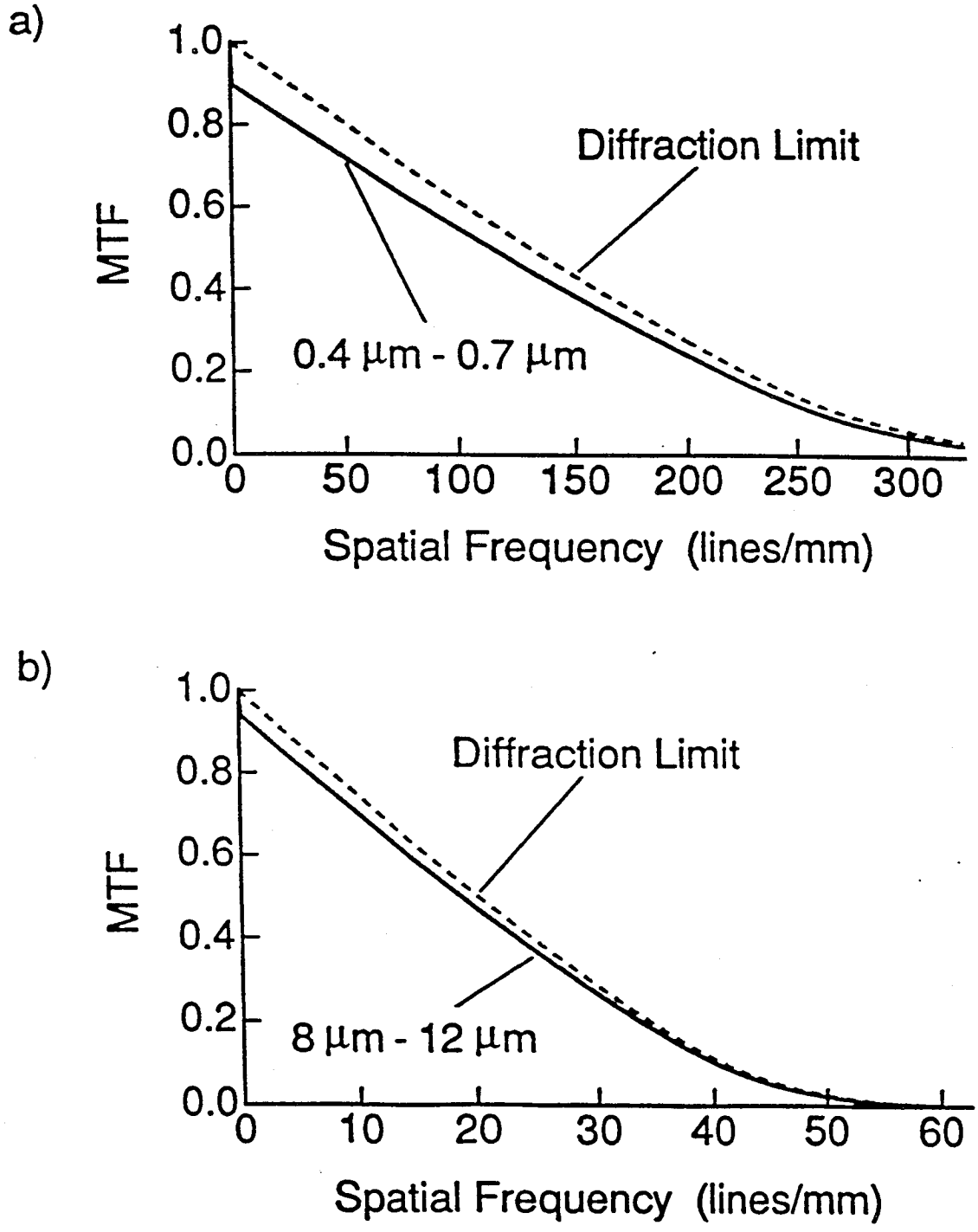

Fig. 4 Polychromatic MTFs for two spectral bands. (a) F/5 system (circular exit pupil) with design wavelength $\lambda_0 = 0.55$ μm and a uniform spectral bandwidth ranging from 0.4 μm to 0.7 μm. The value of $\eta_{int} = 0.914$. (b) F/2 system (circular exit pupil) with design wavelength $\lambda_0 = 10$ μm and a uniform spectral bandwidth ranging from 8 μm to 12 μm. The value of $\eta_{int} = 0.955$.

Table I: Diffractive/Refractive Achromatic Lens Parameters

Total Optical Power of Achromat: Φ_{total}

Lens Powers for Refractive and Diffractive Elements

$$\Phi_{ref} = \frac{\nu_{ref}}{\nu_{ref} - \nu_{dif}} \Phi_{total} \qquad \Phi_{dif} = \frac{\nu_{dif}}{\nu_{dif} - \nu_{ref}} \Phi_{total}$$

Abbe ν-numbers

$$\nu_{ref} = \frac{n(\lambda_0) - 1}{n(\lambda_{short}) - n(\lambda_{long})} \qquad \nu_{dif} = \frac{\lambda_0}{\lambda_{short} - \lambda_{long}}$$

Partial Dispersion

$$P_{ref} = \frac{n(\lambda_{short}) - n(\lambda_0)}{n(\lambda_{short}) - n(\lambda_{long})} \qquad P_{dif} = \frac{\lambda_{short} - \lambda_0}{\lambda_{short} - \lambda_{long}}$$

Secondary Spectrum (Δl_{SAC})

$$\Delta l_{SAC} = \left(\frac{-1}{\Phi_{total}}\right) \frac{P_{ref} - P_{dif}}{\nu_{ref} - \nu_{dif}}$$

Table II: Material Parameters for Hybrid and Doublet Lens Design

Visible (0.486 - 0.656 μm)

Material	ν–number	Partial Dispersion, P
Diffractive	-3.45	0.5962
BK7	64.12	0.6932
F2	36.37	0.7062

Mid-Infrared (3.0 - 5.0 μm)

Material	ν–number	Partial Dispersion, P
Diffractive	-2.00	0.5000
Germanium	101.49	0.6879
Silicon	250.05	0.6701
Zinc Sulfide	112.65	0.4865
Zinc Selenide	179.38	0.6250

Far-Infrared (8.0 - 12.0 μm)

Material	ν–number	Partial Dispersion, P
Diffractive	-2.50	0.5000
Germanium	1001.07	0.7000
Zinc Selenide	58.63	0.4583

Table III: Achromatic Diffractive/Refractive Hybrids and Doublets

Total Optical Power of Achromat: Φ_{total}

Visible (0.486 - 0.656 μm)

Lens	Optical Powers	Secondary Spectrum, Δl_{SAC}
Diffractive/BK7	$\Phi_{dif} = 0.05\ \Phi_{total}$ $\Phi_{BK7} = 0.95\ \Phi_{total}$	$-0.00144\ (1/\Phi_{total})$
F2/BK7	$\Phi_{F2} = -1.31\ \Phi_{total}$ $\Phi_{BK7} = 2.31\ \Phi_{total}$	$0.000468\ (1/\Phi_{total})$

Mid-Infrared (3.0 - 5.0 μm)

Lens	Optical Powers	Secondary Spectrum, Δl_{SAC}
Dif/Germanium	$\Phi_{dif} = 0.02\ \Phi_{total}$ $\Phi_{Ge} = 0.98\ \Phi_{total}$	$-0.00182\ (1/\Phi_{total})$
Dif/Silicon	$\Phi_{dif} = 0.01\ \Phi_{total}$ $\Phi_{Si} = 0.99\ \Phi_{total}$	$-0.000675\ (1/\Phi_{total})$
Dif/Zinc Sulfide	$\Phi_{dif} = 0.02\ \Phi_{total}$ $\Phi_{ZnS} = 0.98\ \Phi_{total}$	$0.000118\ (1/\Phi_{total})$
Dif/Zinc Selenide	$\Phi_{dif} = 0.01\ \Phi_{total}$ $\Phi_{ZnSe} = 0.99\ \Phi_{total}$	$-0.000689\ (1/\Phi_{total})$
Germanium/ Silicon	$\Phi_{Ge} = -0.68\ \Phi_{total}$ $\Phi_{Si} = 1.68\ \Phi_{total}$	$0.000120\ (1/\Phi_{total})$

Table III, (cont'd)

Far-Infrared (8.0 - 12.0 μm)

Lens	Optical Powers	Secondary Spectrum, Δl_{SAC}
Dif/Germanium	$\Phi_{dif} = 0.002\ \Phi_{total}$ $\Phi_{Ge} = 0.998\ \Phi_{total}$	$-0.000199\ (1/\Phi_{total})$
Dif/Zinc Selenide	$\Phi_{dif} = 0.04\ \Phi_{total}$ $\Phi_{ZnSe} = 0.96\ \Phi_{total}$	$0.000682\ (1/\Phi_{total})$
Zinc Selenide/ Germanium	$\Phi_{ZnSe} = -0.06\ \Phi_{total}$ $\Phi_{Ge} = 1.06\ \Phi_{total}$	$-0.000256\ (1/\Phi_{total})$

2.3 Sub-Wavelength Structured Surfaces

Sub-wavelength structured surfaces can be used for two important functions in NASA instrument design: (1) anti-reflection surfaces for windows, domes, detectors, and baffles; and (2) polarization components (linear polarizers and wave plates) for wavelengths ranging from visible to millimeter wavelengths.

To suppress unwanted reflections from optical surfaces, one traditionally uses an anti-reflection coating or a multi-layer stack of thin films. There are a number of difficulties associated with thin-film coatings. For example, the index of refraction for the coating specified for the coating design may not be physically attainable, or the thermal properties of the coating may not be compatible with the substrate material, and so on. Recently, the use of anti-reflective structured (ARS) surfaces have been proposed as a novel alternative to thin-film coatings [13-16].

ARS surfaces add new degrees of freedom to the design of anti-reflective (AR) surfaces. ARS surfaces consist of high frequency, periodic, surface-relief patterns. The period of the surface-relief pattern is small compared to the wavelength of the incident light; hence, the light "sees" an effective (or average) index of refraction that depends on the ratio n_s/n_i, where n_s is the index of refraction of the substrate and n_i is the index of refraction of the incident (or surrounding) medium. Consequently, one can *synthesize* a desired index of refraction for the surface by tailoring the surface structure rather than the chemical or molecular composition. Another feature of ARS surfaces is that they are etched directly into the substrate itself. Consequently, ARS surfaces possess the same thermal and mechanical properties as the substrate itself.

Preliminary results indicate that ARS surfaces can exhibit remarkable anti-reflection properties. It appears that one can fabricate ARS surfaces that are essentially insensitive to the polarization of the incident light, and can function over a broad wavelength band and over a wide range of incidence angles.

An example of the performance that can be achieved is shown in Fig. 5. A multi-step approximation to a continuous 2-D pyramid-type profile, see Fig. 5(a), was analyzed using rigorous coupled-wave theory. Figures 5(b) and 5(c) show the response of 2 (binary), 4, 8, and 16-level dielectric ARS surfaces versus wavelength and angle of incidence, respectively. These profiles were optimized for normal incidence at the design wavelength, λ_0.

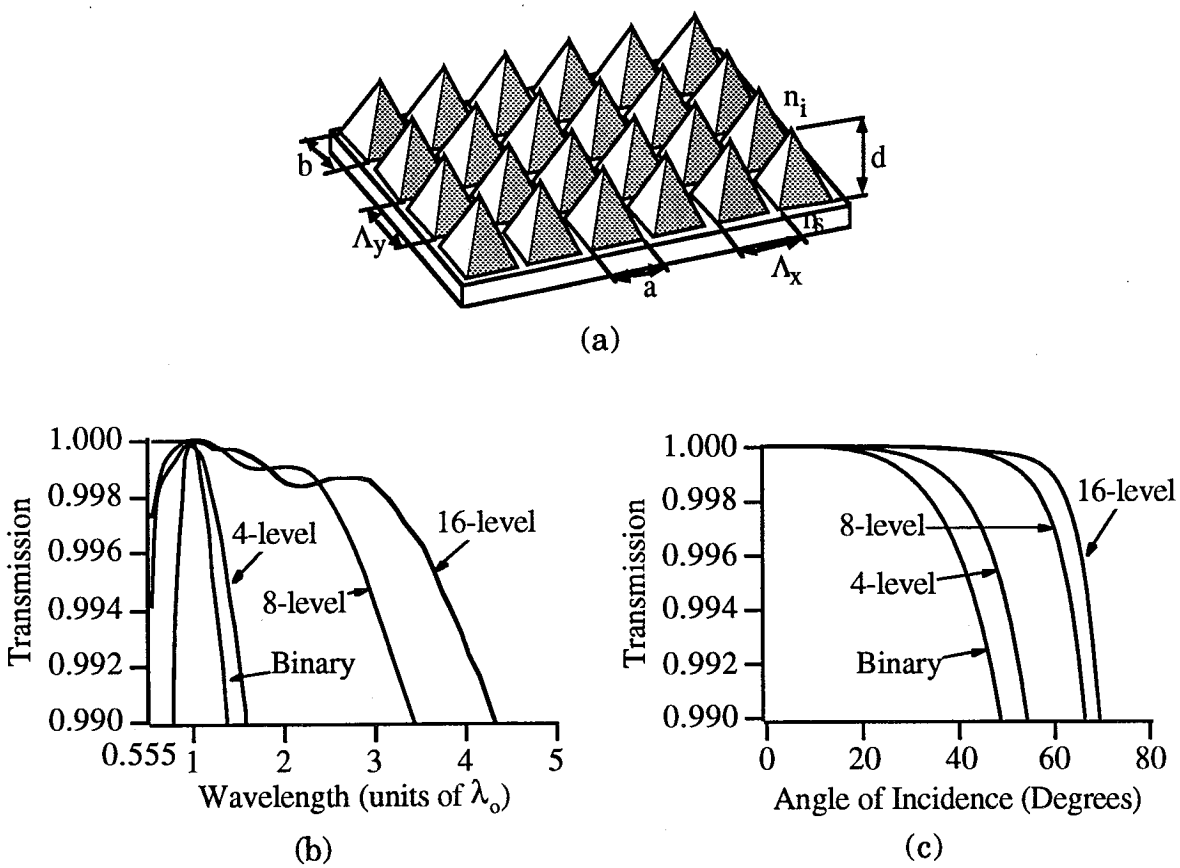

Fig. 5 (a) Two-dimensional continuous pyramid-type profile. To exhibit AR properties, the spatial periods Λ_x and Λ_y of the surface structure must be small compared to the wavelength of the incident light. The height of the surface profile typically ranges from $0.2\lambda_o$ to $1.5\lambda_o$, where λ_o represents design (or center) wavelength. (b) Power transmission coefficient for a stepped-approximation of the continuous 2-D profile versus wavelength. (c) Power transmission of a discrete-step approximation of the continuous 2-D profile versus angle of incidence. In (b) and (c) the incident light is assumed to be randomly polarized, and $\Lambda_x = \Lambda_y = 0.35\lambda_o$.

There are a many of applications that can benefit from ARS surface technology. Transmissive optical elements, such as windows and domes, can utilize ARS surfaces to suppress reflections; these losses can be critical, particularly at infrared and submillimeter wavelengths. Also, absorptive elements, such as infrared detectors and baffles can be designed with ARS surfaces to reduce reflections.

Sub-wavelength structured surfaces can also function as a birefringent material, which can be used for polarization control in optical systems, including linear polarizers and wave plates, and space-variant depolarizers.

Sub-wavelength structured surfaces are likely to play an important role in the design of optical instrumentation for space applications.

2.4 References

1. See, for example, SPIE Proc. Vol. **883**, **1052**, **1136**, **1211**, **1354**, **1507**; also see, special issue of Opt. Eng. **28**, June 1989, SPIE Milestone Series **MS 34** (1991), OSA Tech. Dig. on "Diffractive Optics," April 13-15 (1992).

2. L. d'Auria, J. P. Huignard, A. M. Roy and E. Spitz, Opt. Commun. **5**, 232 (1972); G. J. Swanson and W. Veldkamp, Opt. Eng. **28**, 605 (1989).

3. V. P. Koronkevich, in *Optical Processing and Computing*, H. H. Arsenault, T. Szoplik, and B. Macukow, Eds. (Academic, Boston, 1989), pp. 277-313; W. Goltsos and S. Liu, Proc. SPIE **1211**, 137 (1990).

4. P. P. Clark and C. Londono, Opt. News **15**, 39 (1989); G. M. Morris and D. A. Buralli, Opt. News **15**, 41 (1989); J. A. Futhey, Proc. SPIE **1052** (1989); and M. Reidl and J. T. McCann, Proc. SPIE **1485** (1991).

5. D. A. Buralli and G. M. Morris, Appl. Opt. **30**, 2151 (1991).

6. W. C. Sweatt, J. Opt. Soc. Am. **67**, 803 (1977).

7. W. A. Kleinhans, Appl. Opt. **16**, 1701 (1977).

8. D. Sinclair, OSLO Design Notes, Vol. 1, No. 1, January 1990.

9. D. A. Buralli, G. M. Morris, and J. R. Rogers, Appl. Opt. **28**, 976 (1989).

10. See for example, R. Kingslake, *Lens Design Fundamentals* (Academic, New York, 1978), Chap. 4.

11. C. Londono and P. P. Clark, Proc. SPIE **1354**, 30 (1990).

12. D. A. Buralli and G. M. Morris, "Effects of diffraction efficiency on diffractive lens MTF," To appear in *Applied Optics*, July 1992.

13. R.C. Enger and S.K. Case, "Optical elements with ultrahigh spatial-frequency surface corrugations," *Appl. Opt.* **22**, 3220 (1983).

14. T.K. Gaylord, W.E. Baird, and M.G. Moharam, "Zero-reflectivity high spatial-frequency rectangular dielectric surface-relief gratings," *Appl. Opt.* **25**, 4562 (1986).

15. D. H. Raguin and G. M. Morris, "Anti-reflection structured surfaces for the infrared spectral region," Accepted for publication in *Applied Optics*, July 1992.

16. D. H. Raguin and G. M. Morris, "Analysis of anti-reflection structured surfaces with continuous one-dimensional surface profiles," Submitted to *Applied Optics*, July 1992, in review.

3.0 NASA GEO Documents Reviewed

Information on the design of the various sensors being planned the geostationary earth observatory (GEO) is contained in several of different reports. A list of the reports that were used to ascertain the applicability of diffractive optics technology for the GEO is given below.

NASA Geostationary Earth Processes Spectrometer (GEPS)
Hughes, Conceptual Design Study
Final Report
May 1990

High Resolution Earth Processes Imager (HEPI)
HEPI Phase A Instrument
Observational Systems Division
Jet Propulsion Laboratory
JPL D-7245
February 28, 1990

GeoPlatform High-resolution Interferometer Sounder (GPHIS)
GPHIS Phase A Study
Univ. of Wisconsin and
Santa Barbara Research Center
June 5, 1990

Study of Geoplat Complementarity with NOAA GOES Instruments:
Geoplatform Instrument Studies Final Report
Paul Menzel
July 15, 1990

Lightning Mapper Sensor (LMS)
Final Review (Viewgraphs)
September 18, 1990
Performance Review Documentation
TRW Space and Technology Group

Geostationary Imager Concept Development
Final Report
GE Astro Space
September 25, 1990

Earth Sciences Geostationary Platform
Phase A Study
Solar Total and Spectral Irradiance Monitors
JPL
October 19, 1990

Geostationary Microwave Precipitation Radiometer
Phase A Study Report
JPL
May 1990, Revised January 1991

Geostationary Earth Climate Sensor
GECS Phase A Final Report
Colorado State University &
TRW Applied Technology Division
February 6, 1991

Geostationary Earth Climate Sensor:
Scientific Utility and Feasibility
Colorado State University
Phase A Final Report
July 1991

4.0 Potential Applications of Diffractive Optics Technology

4.1 Overview

Based on the review of the documents listed in Section 3, we have identified several potential applications of diffractive optics. These applications group naturally into the following categories.

Diffractive/Refractive Hybrid Lenses for Aft-Optic Imagers

In many of the instruments that are being planned for the GEO, the output of a broadband reflective telescope is divided into several narrowband and broadband channels. The use of a diffractive/refractive hybrid lens in the aft-optic imager offers the possibility to reduce the aft-imager weight significantly (in some cases by more than a factor of two) and can provide performance comparable to that of aspheric optical systems without having to use aspheric surfaces; this can reduce system costs. With hybrid lenses, mechanical mounts can be simplified and stability can also be better than with all-refractive lens systems. A diffractive/refractive hybrid lens should be applicable to aft-optic imagers in which the spectral bandwidth $\Delta\lambda/\lambda \leq 0.5$.

A preliminary design for an aplanatic, diffractive/refractive aft-imager is described in Section 5.1.

Diffractive Telescopes for Narrowband Imaging

With narrowband illumination, an all-diffractive telescope can provide excellent imaging over wide fields of view. Diffractive lenses exhibit two unique properties that make them excellent candidates for use in narrowband telescope design. First, by varying the zone spacing of the diffractive lens, one can create an aspheric wavefront without having to use aspheric surfaces. Second, a diffractive lens does not introduce any Petzval curvature into an optical system. Hence, if one can eliminate astigmatism, the resulting image will be formed on a flat surface. By using diffractive, rather than refractive lens elements, our preliminary calculations, see Section 5.2, indicate that it should be possible to achieve imaging performance comparable to the refractive system and reduce the weight of the telescope by approximately a factor of two.

Sub-Wavelength Structured Surfaces for Anti-Reflection and Polarization Control

Sub-wavelength structured (SWS) surfaces can play an important role in many of the instruments planned for the GEO. Anti-reflection structured (ARS) surfaces can provide excellent anti-reflection (AR) properties over broad spectral bands and wide fields

of view. Potential applications include ARS surfaces for windows, optical detectors, solar cells, and baffles for wavelengths ranging from the near-infrared to the sub-millimeter-wave region. SWS surfaces can also be used for polarization control, including large aperture linear polarizers, wave plates, and space-variant wave plates for depolarization of optical instruments.

Aberration Compensation for Reflective Imaging Systems

Surface-relief diffractive wave plates can be used to used to compensate for aberrations in reflective optical systems. Two different implementations are analyzed: (1) the use of a diffractive (or binary) optics Schmidt plate to eliminate spherical aberration in telescopes, and (2) a diffractive element on the surface of a spherical reflector for aspheric wavefront generation. Preliminary optical designs for these implementations are discussed in Sections 5.3 and 5.4.

4.2 Specific GEO Sensors

4.2.1 Lightning Mapper Sensor (LMS)

The Lightning Mapper Sensor (LMS) appears to be a candidate for insertion of diffractive optics technology. In the LMS, a narrowband telescope with a center wavelength of 777.4 nm is required to operate over a ± 4.7 degree field of view. The current telescope design consists of three zinc-sulfide (ZnS) elements — two of the elements serve as the objective and eyepiece for the telescope, and the third element is used as a field flattener to reduce the effects of Petzval field curvature. The total weight of the current design is 938 grams.

By using diffractive, rather than refractive lens elements, our preliminary calculations indicate that it should be possible to achieve imaging performance comparable to the refractive system while significantly reducing the weight of the telescope.

As discussed above in Section 2.1, diffractive lenses exhibit two unique properties that make them excellent candidates for use in narrowband telescope design. First, by varying the zone spacing of the diffractive lens, one can create an aspheric wavefront without having to use aspheric surfaces. Second, a diffractive lens does not introduce any Petzval curvature into an optical system. Hence, if one can eliminate astigmatism, the resulting image will be formed on a flat surface. This is in contrast to well-corrected refractive optical systems, which can have a flat field in only one meridian.

A preliminary optical design for an all-diffractive telescope, suitable for application in the LMS, is described in Section 5.2. In contrast to a refractive lens where the thickness (or

weight) of an element is determined primarily by the surface curvatures, the thickness (or weight) of the substrate for a diffractive lens is based solely on the mechanical/environmental requirements imposed by the application. The substrate must simply be thick enough to be mechanically stable during deployment and operation. For example, if it is determined that a substrate of 5-mm thickness provides sufficient mechanical stability, then the total weight of the lens elements for the diffractive telescope will be only 577 grams, compared to 938 grams obtained for the comparable refractive telescope design.

Also, it appears that anti-reflection structured (ARS) surfaces may be useful in the construction of the Barr multi-cavity filter.

4.2.2 NOAA GOES N Imager

Diffractive optical elements can be used in the design of optical systems that operate with broadband illumination. As discussed in Section 2.2, to achieve good performance over a broad spectral band, one must use combinations of refractive and diffractive elements. Generally to obtain achromatic operation in the visible spectral region, approximately 95% of the optical power of a diffractive/refractive hybrid lens resides in the refractive component. The remaining 5% of the optical power resides in the diffractive element. Higher-order phase terms can also be incorporated into the diffractive element to generate the aspheric wavefronts needed to obtain good image quality over a wide field of view. Both the design and performance of a diffractive/refractive lens operating with broadband illumination are dependent on the spectral bandwidth of the illumination. Generally, however, we have found that an achromatic hybrid lens can be expected to work reasonably well for spectral bandwidths in which $\Delta\lambda/\lambda \leq 0.5$.

There are numerous aft-imagers that are planned for the GEO that fall within this $\Delta\lambda/\lambda \leq 0.5$ bandwidth constraint. For example, in the GOES N imager, which provides multi-spectral imaging of the full earth disk for mass and motion field determinations, the spectrum of the incident light is divided into seven channels:

$0.55\ \mu m \leq \lambda \leq 0.75\ \mu m$	$\Delta\lambda/\lambda = 0.31$
$3.8\ \mu m \leq \lambda \leq 4.0\ \mu m$	$\Delta\lambda/\lambda = 0.05$
$6.5\ \mu m \leq \lambda \leq 7.0\ \mu m$	$\Delta\lambda/\lambda = 0.07$
$7.1\ \mu m \leq \lambda \leq 7.5\ \mu m$	$\Delta\lambda/\lambda = 0.05$
$10.5\ \mu m \leq \lambda \leq 11.2\ \mu m$	$\Delta\lambda/\lambda = 0.06$
$11.5\ \mu m \leq \lambda \leq 12.5\ \mu m$	$\Delta\lambda/\lambda = 0.08$
$13.1\ \mu m \leq \lambda \leq 13.6\ \mu m$	$\Delta\lambda/\lambda = 0.04$

It appears that the aft-imagers of GOES N could benefit from the use of diffractive/refractive hybrid lenses. A preliminary design for an aplanatic, aft-imager lens is described below in Section 5.1.

4.2.3 GeoPlatform High-resolution Interferometer Sounder (GPHIS)

GPHIS is a high resolution infrared interferometer with a spectral range from 3.7 $\mu m \leq \lambda \leq 16.1\ \mu m$ ($\Delta\lambda/\lambda = 1.25$). The spectral range is divided into 5 broadbands and five narrow bands. The five broadband channels are:

Band 5	$3.7\ \mu m \leq \lambda \leq 4.3\ \mu m$	$\Delta\lambda/\lambda = 0.15$
Band 4	$4.3\ \mu m \leq \lambda \leq 5.9\ \mu m$	$\Delta\lambda/\lambda = 0.31$
Band 3	$5.9\ \mu m \leq \lambda \leq 9.0\ \mu m$	$\Delta\lambda/\lambda = 0.42$
Band 2	$9.0\ \mu m \leq \lambda \leq 10\ \mu m$	$\Delta\lambda/\lambda = 0.11$
Band 1	$10\ \mu m \leq \lambda \leq 16.1\ \mu m$	$\Delta\lambda/\lambda = 0.47$

Again, based on the values of the bandwidth ($\Delta\lambda/\lambda$) of various aft-imager bands, it appears that GPHIS is also a candidate for diffractive/refractive hybrid lenses.

4.2.4 High Resolution Earth Processes Imager (HEPI)

HEPI is a 0.75-m telescope imager, which provides high resolution spatial images in the spectral range from $0.3\ \mu m \leq \lambda \leq 2.4\ \mu m$. The spectrum is divided into three aft-imager sections:

UV:	$0.3\ \mu m \leq \lambda \leq 0.4\ \mu m$	$\Delta\lambda/\lambda = 0.29$
VIS:	$0.4\ \mu m \leq \lambda \leq 0.9\ \mu m$	$\Delta\lambda/\lambda = 0.77$
LWIR:	$0.9\ \mu m \leq \lambda \leq 2.4\ \mu m$	$\Delta\lambda/\lambda = 0.91$

Based on the bandwidth of the aft-imagers, it appears that the visible (VIS) and long wave infrared channels (LWIR) would not be suitable for diffractive/refractive hybrids. However, the UV channel could indeed benefit from the use of a hybrid lens. In this spectral region ($0.3\ \mu m \leq \lambda \leq 0.4\ \mu m$), optical materials are rather limited, which makes the design of achromatic systems difficult. A unique feature of diffractive/refractive hybrid lenses is that they do not require the use of exotic materials. Achromatization over the spectral bandwidth of $\Delta\lambda/\lambda = 0.29$ should be possible using only one material (e.g. fused silica) in conjunction with the surface-relief diffractive element. It is also possible to add aspheric terms in the diffractive lens; hence, one can obtain good imaging over a wide field of view without having to use aspheric refractive surface profiles.

In the HEPI report [High Resolution Earth Processes Imager (HEPI), HEPI Phase A Instrument, JPL D-7245, page 27] it is stated that "Depolarization of the optical beam in the HEPI instrument is not practical since the best place to locate a depolarizing element is in the collimated space in front of all the optical elements. It is not likely that a depolarizer can be made large enough to fit the size of the beam at that point. "

Note, however, by using a polarizer based on SWS surfaces, it is highly likely that one can construct a large-aperture, space-variant polarizer, see the discussion in Section 2.4.

4.2.5 Geostationary Earth Processes Spectrometer (GEPS)

GEPS divides the spectrum of the incident light into 37 spectral bands and employs three aft-imagers. The spectral bands of the aft imagers are:

VIS/NIR:	$0.32\ \mu m \le \lambda \le 0.94\ \mu m$	$\Delta\lambda/\lambda = 0.98$
SW/MWIR:	$1.24\ \mu m \le \lambda \le 4.565\ \mu m$	$\Delta\lambda/\lambda = 1.15$
LWIR:	$6.72\ \mu m \le \lambda \le 14.24\ \mu m$	$\Delta\lambda/\lambda = 0.72$

Because the spectral bandwidths of the aft-imagers are rather large, it is doubtful that hybrid lenses will work very well in GEPS.

However, as in HEPI, low polarization sensitivity is required for high radiometric accuracy [NASA Geostationary Earth Processes Spectrometer (GEPS), Hughes, Conceptual Design Study, May 1990, p. 5]. Again, SWS surfaces may provide a means to eliminate polarization effects introduced by the other optical elements.

4.2.6 Geostationary Imager Concept Development

The optical system consists of a telescope, a field sampling mirror, imaging optics, spectral beam splitters, and a detector array. In the report [Geostationary Imager Concept Development, Final Report, GE Astro Space, September 25, 1990, p. 30], it is noted that a Schmidt plate could be used to reduce the spherical aberration in the telescope, however, a refractive phase plate is difficult to make.

It appears that a diffractive Schmidt phase plate or a diffractive aberration corrector incorporated in the surface of the mirror may provide an effective means to eliminate telescope aberrations, see discussion of optical designs in Sections 5.3 and 5.4.

Also, on page 32 of the GE report, it is observed that "An issue to be addressed is performance of AR (anti-reflection) coatings over a broad 0.4 to 2.4 micron band." It is possible that ARS surfaces can provide good anti-reflection properties over this spectral band, see discussion in Section 2.3.

4.2.7 Solar Total and Spectral Irradiance Monitors (TIM and SIM)

With TIM and SIM, the goal is to understand the implications of solar irradiance variability for weather and climate, and for solar physics. The spectral range for TIM is from the far UV to the far IR with uniform sensitivity. The spectral range for SIM is from 0.35 to 4.0 μm. The TIM system consists of a radiometer/detector design (little or no optics). The SIM system is currently comprised of three sets of prism spectrometers. Each set is composed of a "visible" (VSIM) and an "infrared" (ISIM) spectrometer.

Nowhere in the report [Earth Sciences Geostationary Platform, Phase A Study, Solar Total and Spectral Irradiance Monitors, October 1990] is the use of prisms in the spectrometer design justified. Grating spectrometers should be considered. Given the current state of the art in diffractive element fabrication, it is possible to incorporate aberration correction in the design of the grating spectrometers, which can significantly reduce the size and weight of the spectrometers.

Also, it is noted in the report that the primary losses are reflection losses on mirror and prisms surfaces. Again, ARS surfaces offer the possibility of reducing surface reflections over broad wavelength bands, and also minimizing polarization effects.

The SIM system provides an excellent opportunity to demonstrate the benefits that diffractive optics technology can offer for reducing the complexity, size, weight, and cost of a space-optics instrument.

4.2.8 Geostationary Microwave Precipitation Radiometer (GMPR)

The GMPR provides microwave images for meteorology. The microwave radiation is divided into seven frequency bands ranging from 37 to 220 GHz. It employs a 4-meter parabolic antenna which has an efficiency greater than 90%.

GMPR does not appear to offer any opportunities for insertion of diffractive optics.

4.2.9 Geostationary Earth Climate Sensor

The earth climate sensor will provide a radiation budget for the earth. The sensor covers the spectral range from $0.2\ \mu m \leq \lambda \leq 100\ \mu m$, in which $\Delta\lambda/\lambda = 1.99$. The spectrum is divided into three spectral channels:

Channel 1	$0.2\ \mu m \leq \lambda \leq 4.0\ \mu m$	$\Delta\lambda/\lambda = 1.81$
Channel 2	$4.0\ \mu m \leq \lambda \leq 100\ \mu m$	$\Delta\lambda/\lambda = 1.85$
Channel 3	$0.2\ \mu m \leq \lambda \leq 100\ \mu m$	$\Delta\lambda/\lambda = 1.99$

Because the spectral range in each channel is so large, diffractive optics technology is simply not suitable for this instrument.

5.0 Optical System Design using Diffractive Optical Elements

5.1 Design of a Hybrid Diffractive/Refractive Aft-Imager

Aft-imagers are used in several of the proposed instruments aboard the Geostationary Earth Observatory to image light from a main telescope onto a detector after spectral filtering. These imagers are used to increase the speed of the optical beam onto a detector, which allows a smaller detector to be used and thereby increases the signal-to-noise ratio. This is very important in systems that are limited by detector noise.

Diffractive lenses can be used in the design of optical systems that operate with broadband illumination. To achieve good performance over a broad spectral band, one must use combinations of refractive and diffractive elements. To obtain achromatic performance 95-99% of the optical power must reside in the refractive element and the remaining power resides in the diffractive element. Higher-order phase terms can also be incorporated into the diffractive element to generate aspheric wavefronts. Both the design and the performance of a diffractive/refractive lens operating with broadband illumination are dependent on the spectral bandwidth of the illumination. Generally, however, we have found that an achromatic hybrid lens can be expected to work reasonably well for spectral bandwidths in which $\Delta\lambda/\lambda \leq 0.5$. There are numerous aft-imagers planned for the GEO that fall within this bandwidth constraint.

Typically, aplanatic lenses are used as aft imagers because they will increase the speed of a converging cone without adding spherical aberration or coma. A lens will only be aplanatic under a particular set of conditions. It has been shown[1] that the aplanatic points of a surface i and o are the conjugates that satisfy the condition that the angles I and U in Fig. 6 are equal.

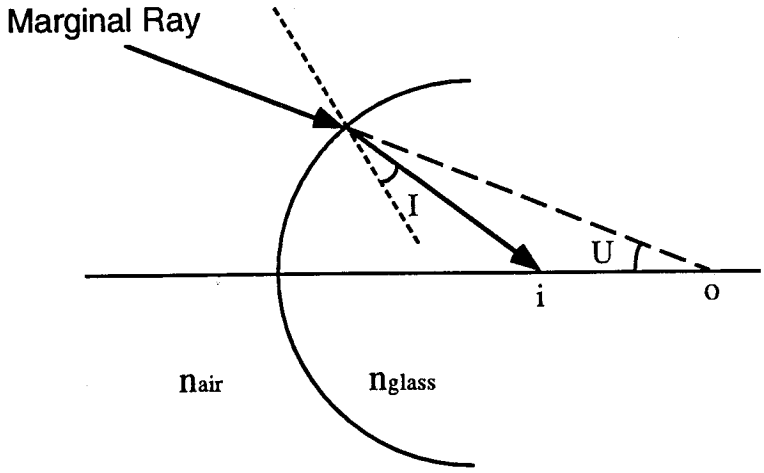

Fig. 6. The aplanatic points of a surface are the points i and o that satisfy the condition that I=U.

[1] R. Kingslake, *Lens Design Fundementals* (Academic Press, Orlando, 1978)

The angle I is the angle of refraction of the marginal ray and the angle U is the angle between the incident marginal ray and the optical axis. The points i and o are the image and object conjugate points. At these conjugate points the surface introduces no spherical aberration or coma.

Spherical aberration of a lens is independent of field position and is the only on-axis aberration. Coma is an aberration that increases with field height. Imaging onto detectors then divides into two cases; on-axis imaging and wide field imaging. The case of imaging onto a single-element, on-axis detector requires correction of only spherical aberration. Detector arrays, used in wide-field imaging, require correction of both spherical aberration and coma.

An aplanatic singlet is made by making the front surface aplanatic and the rear surface perpendicular to the marginal ray. The increase in beam speed of an aplanat is related to the refractive index.[2] For example, the AVHRR lens[3] uses a germanium aplanatic lens (refractive index of 4.00) to increase the cone angle incident on the detector from f/2.6 to f/0.65. This beam is incident onto a single-element, on-axis, square detector 0.0068 inches in size.

Using aplanats with large cone angles requires an extremely large first surface curvature. The large curvature results in large reflection losses in the extreme rays and a reduction in the field-of-view. The AVHRR aplanat is shown in Fig. 7.

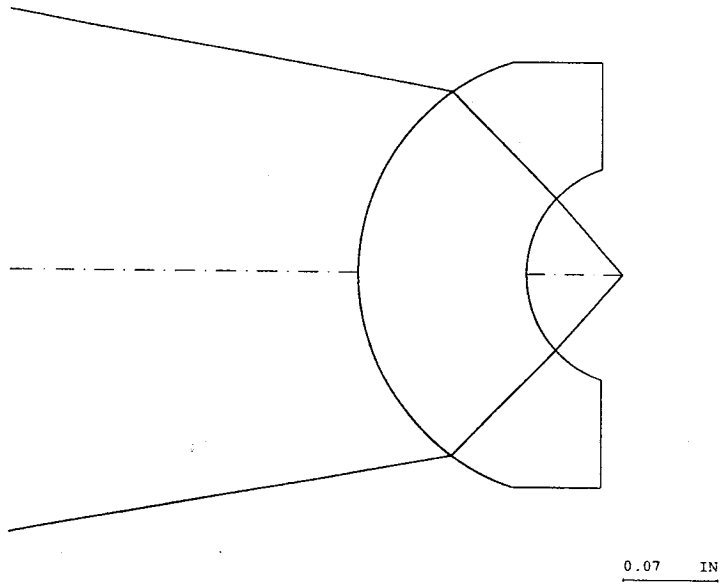

Fig. 7. Aplanat used in the AVHRR system. The extreme curvature of the front surface results in large reflection losses of the extreme rays.

[2] W.T. Welford, *Aberrations of Optical Systems* (Hilger, Bristol, 1986).
[3] Ron Koczor, Private communication, June 11, 1992.

Uncoated, the reflection losses of the extreme rays are 88% through the lens. 81% of the light is lost at the first surface alone. Both the large incident angles and the high index of refraction contribute to these losses. These losses can be reduced using anti-reflection coatings, but the coatings must be optimized for a large incident angle, typically at 50-60°. It is also difficult to apply these coatings to extremely curved surfaces. Even with AR coatings, the reflection losses can be substantial. The problem results in vignetting or reduction in the field-of-view.

In the case of aplanatic imaging, both coma and spherical aberration must be corrected. If the aplanatic condition is to be satsified, the only way to reduce reflection losses is to reduce the curvature of the front surface. This can only be accomplished by splitting the required power over more than one surface.

To reduce the incident angle, a second element can be used to form an aplanatic doublet. A zinc sulfide aplanatic doublet is shown in Fig. 8.

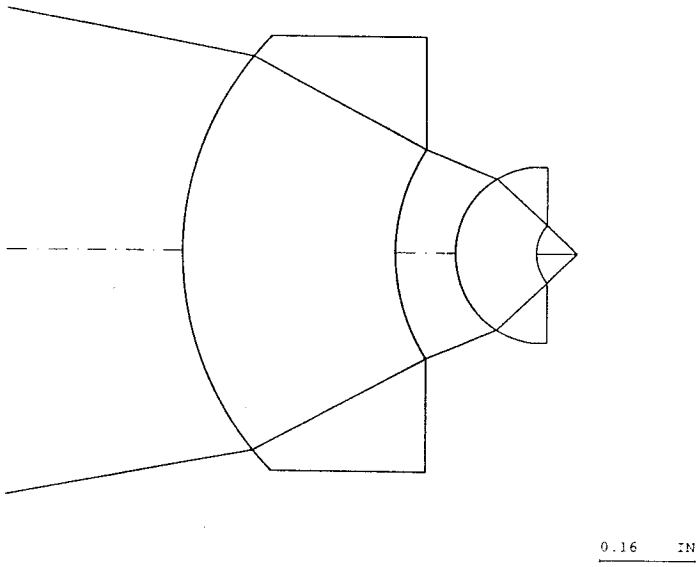

Fig. 8. Aplanatic doublet for use as a wide-field aft-imager. A diffractive lens has been placed on the front of the first surface.

The doublet is made from two ZnS lenses with a weak diffractive element on the front surface of the first element. The diffractive lens is used to correct chromatic aberrations of the doublet. The on-axis performance of the aplanatic doublet is shown in Fig. 9.

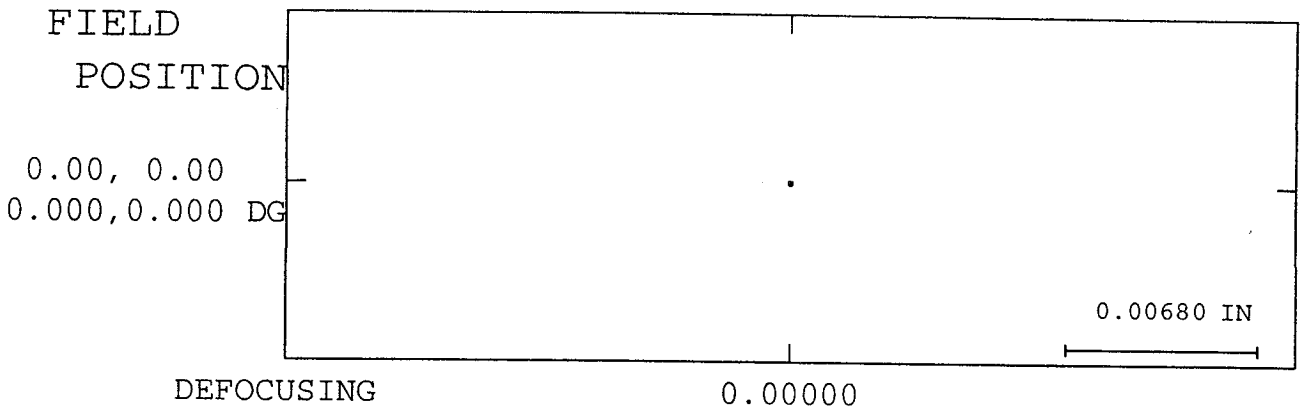

Fig. 9. On-axis performance of the aplanatic doublet.

The on-axis spot size of the doublet is well below the detector size of the AVHRR system. The combined uncoated reflection loss of the doublet is 77.5% for the extreme rays. While this represents a slight reduction in surface reflection losses over the present design, it is not particularly significant.

However, since the AVHRR lens is to be used as an on-axis imager, it is only spherical aberration, not coma, that limits the performance of the system. Since coma correction is not required, the spherical aberration can be corrected by using an aspheric surface. These aspheric terms can be added to a spherical surface by using a diffractive optical element which contains the higher-order phase terms. By using aspheric terms to correct the spherical aberration, the surface curvatures can now be decreased, which in turn reduces the reflection losses.

Using a diffractive lens in combination with a refractive element, a hybrid aft-imager was designed to be used in place of the AVHRR aplanat. This hybrid aft-imager is shown in Fig. 10.

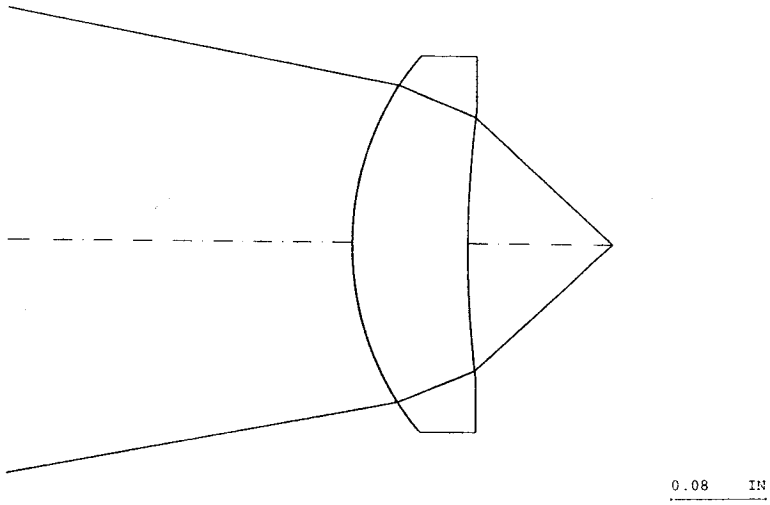

Fig. 10 Hybrid diffractive/refractive aft-imager.

This imager consists of a single ZnS element with a diffractive lens on the front surface. The diffractive lens is used to provide color correction and the aspheric terms required to correct the spherical aberration. The incident beam is f/2.6 and the beam incident on the detector plane is f/0.64. The performance of the hybrid element over the 11.5-12.5 μm wavelengths can be seen in the spot diagram shown in Fig. 11.

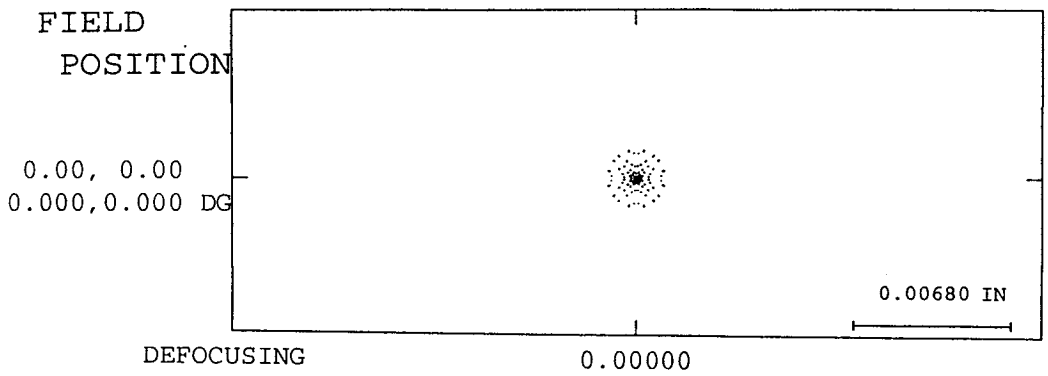

Fig. 11 On-axis performance of the hybrid aft-imager. The scale is the same size as the single-element detector.

The scale bar in the lower right hand corner of the plot is the same as the size of the single element detector, namely, 0.0068 inches. Note that the on-axis spot size is smaller than the detector size.

The reflection losses for the uncoated lens in Fig. 10 is 26% at the extreme rays. This is substantially less than the losses for the germanium aplanat. Anti-reflection coatings will reduce these losses even further. Since the surface curvatures are reduced from that of the germanium aplanat, AR coatings will be easier to apply and can be optimized for a smaller incidence angle.

Comparing the reflection losses of the extreme rays of the hybrid aft-imager and the AVHRR aplanat, the losses of the hybrid aft-imager are 26% and the losses of the AVHRR aplanat are 88%. This is a large improvement. The on-axis performance of the hybrid aft-imager is not as good as the aplanat but the spot size is still well below the size of the detector element.

The use of hybrid diffractive/refractive lenses as aft-imagers, may provide a better solution than refractive aplanatic lenses. The diffractive element provides the extra degrees of freedom needed to correct spherical aberration, there by relaxing the constraints on the surface curvatures. Lower reflection losses are the result of reducing the surface curvatures.

5.2 An All-Diffractive Telescope for the Lightning Mapper Sensor

Diffractive optics are well suited for use in systems utilizing monochromatic illumination. Using monochromatic light, all-diffractive designs can yield superior performance using fewer elements and reduced weight. The Lightning Mapper Sensor may greatly benefit from diffractive optics technology. This system is a narrowband design used to detect the O_2 triplet at 777.4 nm over a ±4.7° field of view. The narrow bandwidth of the system is obtained by using a interference filter. The field is image onto a 640x400 x2 CCD detector array with a pixel size of 37 μm square.

The current telescope design[4] uses three zinc sulfide (ZnS) elements as shown in Fig. 12.

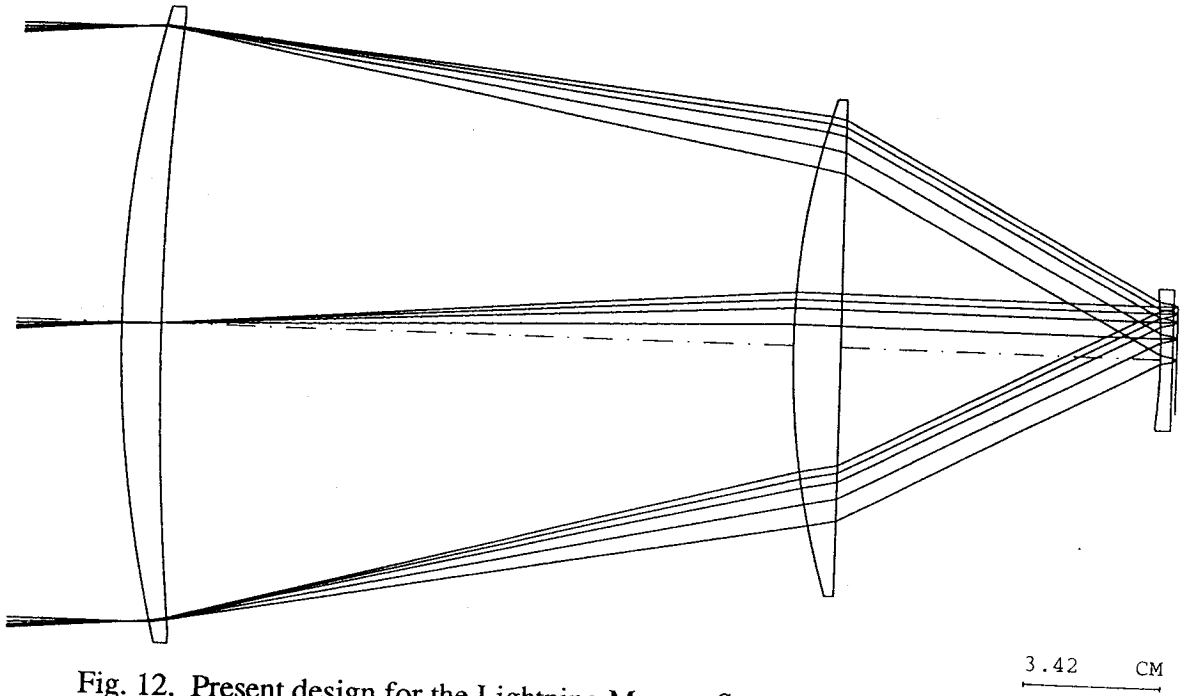

Fig. 12. Present design for the Lightning Mapper Sensor telescope.

The present design uses a two element objective with a field flattener to correct Petzval field curvature. The first surface of the objective lens has a -0.2 conic constant with aspheric terms. The second lens is a plano-convex lens. The entrance pupil diameter is 15.0 cm and the system focal length is 16.4 cm. The combined weight of the three ZnS elements used in the system is 937.9 grams. The spot size diagram in Fig. 13 shows the spot size to be well below 37 μm.

---

[4] Lightning Mapper Sensor (LMS) Final Review (Viewgraphs). Performance Review Documentation. TRW Space and Technology Group, September 18, 1990.

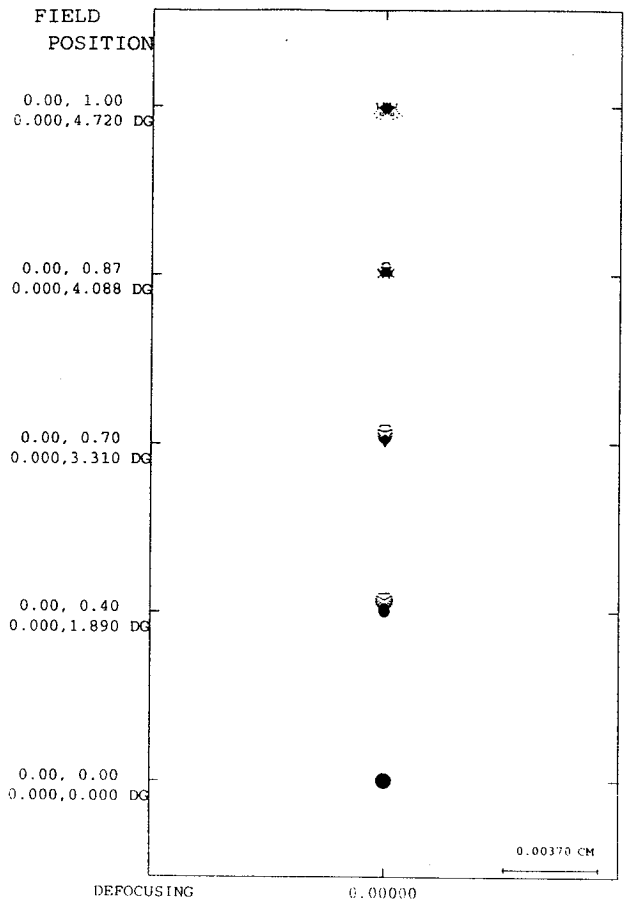

Fig. 13. Spot diagram for the LMS telescope.

The encircled energy plot in Fig. 14 shows that more than 90% of the energy for a spot at each field angle is contained within 15 μm.

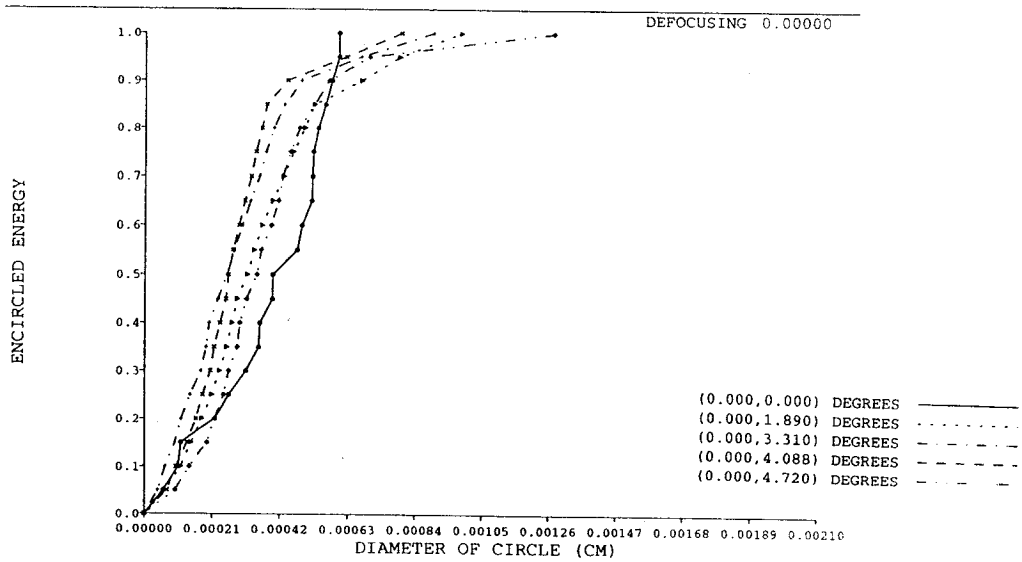

Fig. 14. Encircled energy plot for the present design of the LMS telescope.

An all-diffractive design, suitable for use in the LMS telescope, was generated. This preliminary design has several advantages over the refractive design. Performance is comparable to the refractive design and the weight is significantly reduced. This reduction in weight is possible because, unlike a refractive lens, the performance of a diffractive lens does not depend on the difference in surface curvatures and thus the volume and weight of the glass.

The all-diffractive LMS telescope design is shown in Fig. 15.

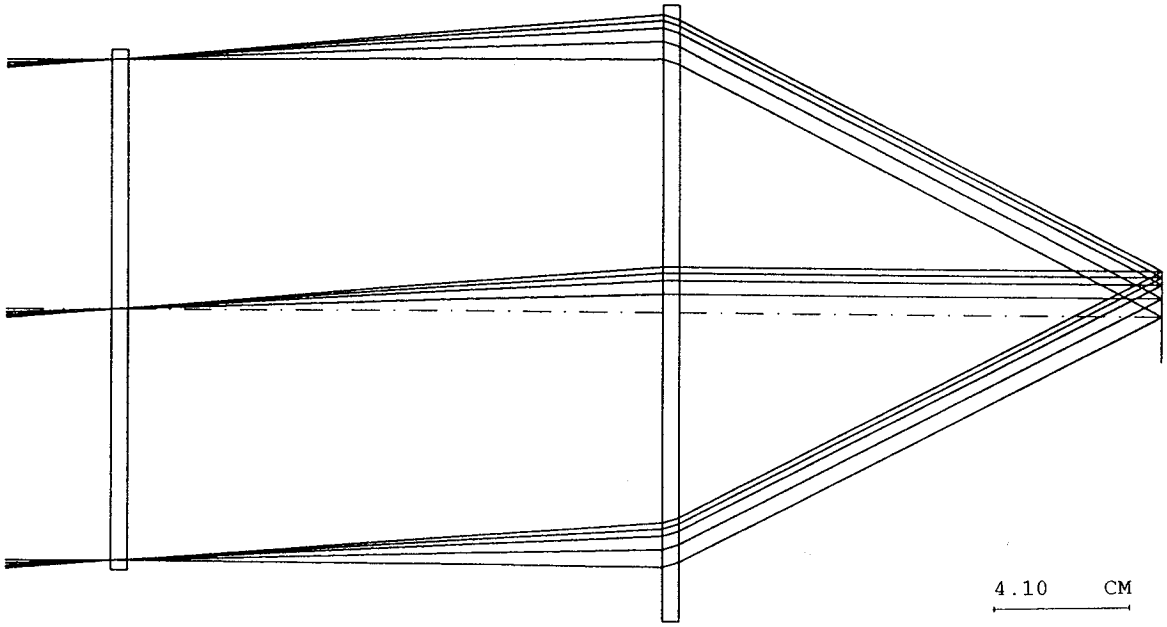

Fig. 15. All-diffractive Lightning Mapper Sensor telescope design.

This design uses two diffractive lenses on spherical BK7 substrates to produce a system focal length of 16.4 cm and an entrance pupil diameter of 15 cm. The first element is an f/11.4 aspheric lens and the second is an f/0.9 spherical lens. A field flattener is not required for this design because diffractive optics inherently do not contribute to Petzval field curvature. Diffractive optics also have the advantage of being able to generate an aspheric element without having to use an aspheric surface. This is done by varying the zone spacing of the diffractive lens.

The weight of the all-diffractive LMS system is 576.6 grams assuming 5 mm thick substrates. Since the performance of the system does not depend on the type or volume of the glass, only the mechanical properties need be considered in determining the appropriate thickness of the glass. The weight of the system would then depend linearly on the thickness.

The performance of the all-diffractive LMS telescope is shown in Figs. 16 and 17.

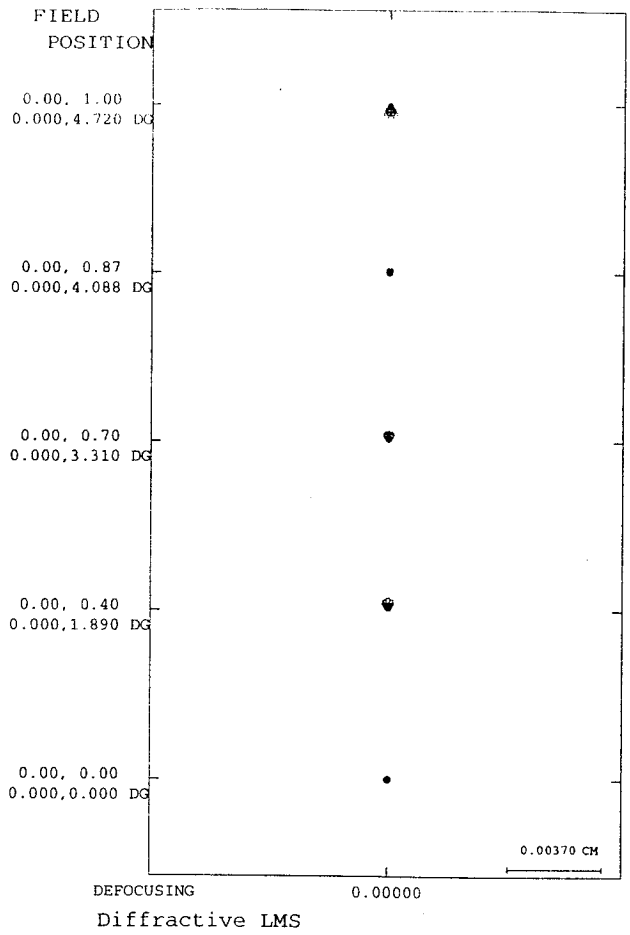

Fig. 16. Spot size diagram of the all-diffractive LMS telescope.

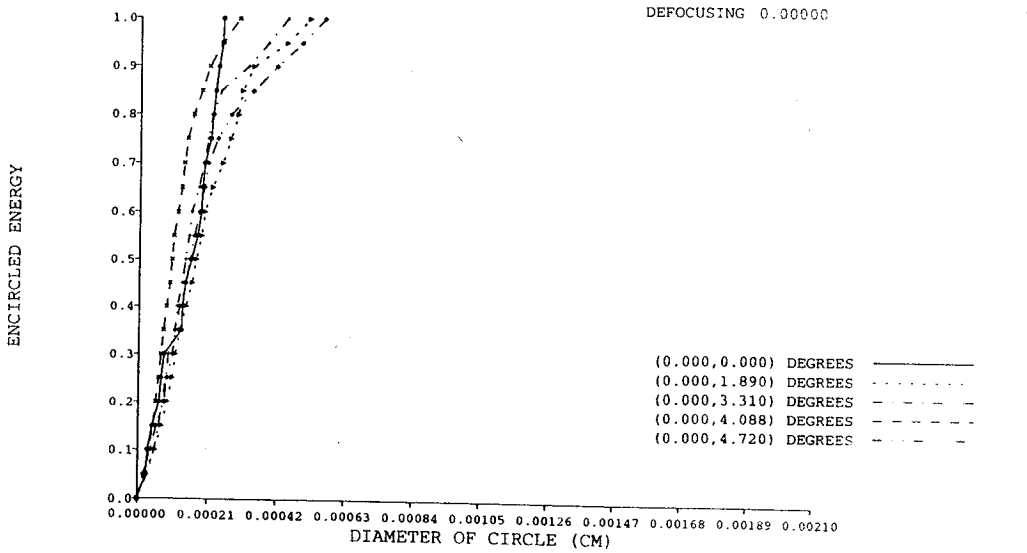

Fig. 17. Encircled energy plots for the all-diffractive LMS telescope.

The spot diagrams, shown in Fig. 16, show the spots to be about 5 μm over the entire field. The CCD pixel size is 37 μm. The encircled energy plots show that over 90% of the energy for each spot is contained within a 4 μm circle. The monochromatic performance is thus much better for the all-diffractive design than for the present design.

The zone spacings of the two diffractive lenses were calculated. The first element has a minimum zone spacing of 460 μm; these zone spacings can be easily achieved using present fabrication technology. The second element is much faster and the zone spacing drops to 1.4 μm; this zone spacing is obtainable using present state-of-the-art technology.

The monochromatic performance of the all-diffractive LMS telescope design is better than that of the present LMS design over the entire field of view. The all-diffractive design has smaller spot sizes meaning there is more energy in a smaller spot than the present LMS design. The weight of the all-diffractive design is 576.6 grams using 5 mm thick substrates where the present design weighs 937.9 grams using ZnS lenses. Unlike the present design, the all-diffractive design obtains the required aspheric wavefront using terms in the phase polynomial and does not require an aspheric substrate to obtain this level of performance. Fabrication of the required diffractive lenses is possible using present technology.

5.3 Diffractive Schmidt Plates for Reflective Telescopes

Reflective telescopes are widely used in instruments because larger elements can be made, they are free from chromatic aberrations and they naturally fold the system into a more compact unit. While spherical surfaces are easy to fabricate, they contribute large amounts of spherical aberration, which prevents their use in most telescope systems. Figure 18 shows an f/1, 200 mm focal length spherical mirror. The performance of this system is shown in Fig. 19.

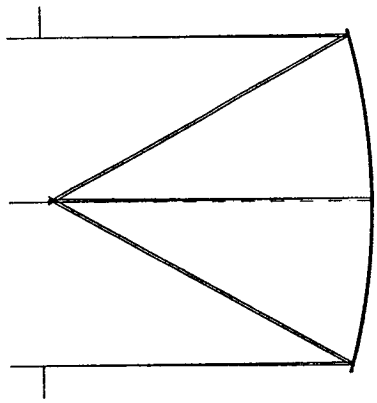

Fig. 18. System layout of an f/1, 200-mm focal length mirror.

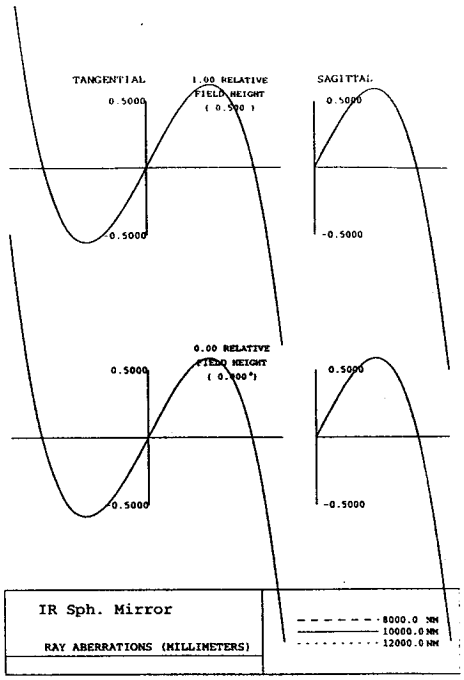

Fig. 19. Ray intercept plot of a f/1, 200-mm focal length mirror. Spherical aberration is the primary aberration.

There are three ways that spherical aberration can be reduced. One way is to use parabolic, ellipsoidal or aspheric mirrors, however, the difficulty is that these non-spherical surfaces are much harder to fabricate than spherical surfaces. A second way is to place an aspheric corrector plate in front of the system in a configuration similar to a Schmidt camera. While large Schmidt systems have been used, making large refractive elements adds complexity and risk.[5]

Diffractive optics offer a third possibility in allowing spherical mirrors to be used in telescope systems operating over a limited bandwidth. Because diffractive a diffractive optical element obtains its performance from surface structure, fabrication methods are the same for generating a simple spherical phase profile and a phase profile containing higher order terms. We have investigated the possibility of using a diffractive Schmidt corrector plate to correct the spherical aberration of a spherical mirror. These diffractive corrector plates can be fabricated on flat substrates. Figure 20 shows a spherical mirror system with a diffractive Schmidt plate. It is an f/1 system with a 200 mm focal length used over a wavelength range from 8-12 μm.

---

[5]Geostationary Imager Concept Development Final Report (Viewgraphs), GE Astro Space, September 25, 1990

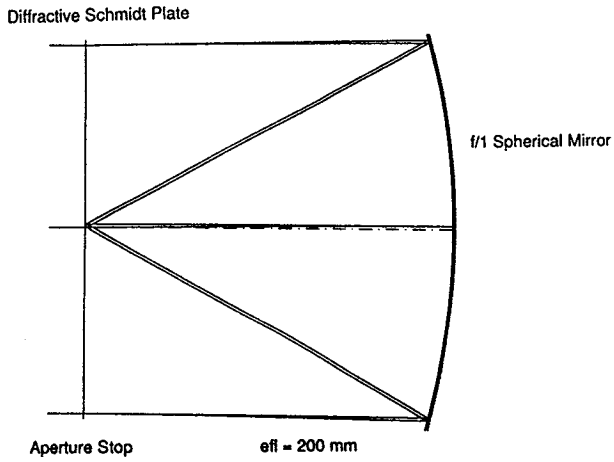

Fig. 20. Diffractive Schmidt corrector plate used with a spherical mirror.

The ray-intercept plots in Fig. 20 show that the aspheric terms of the corrector plate have corrected the spherical aberration of the system improving the performance over the spherical mirror.

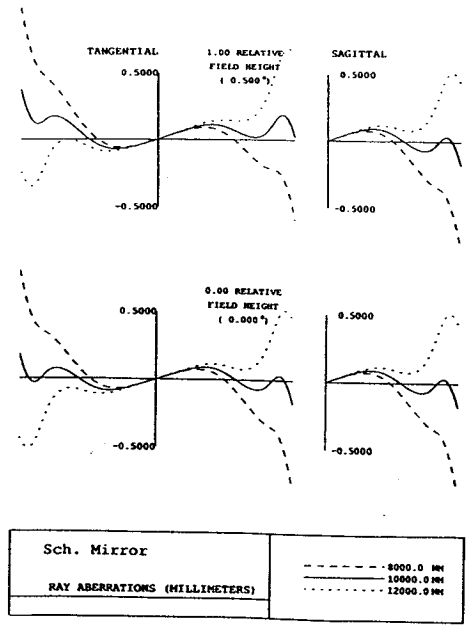

Fig. 21. Performance of a diffractive Schmidt mirror system. The performance is improved over the uncorrected mirror.

Adding a diffractive element to a mirror will produce chromatic aberrations. These chromatic aberration effects may be balanced by using refractive elements in the aft-imaging section of the telescope.

The minimum zone spacing of the aspheric corrector plate is 640 μm. Fabrication of this plate is easily accomplished using present technology.

The diffractive Schmidt mirror system can be a method of improving the performance of a spherical mirror without requiring the fabrication of a refractive aspheric correcter plate. In combination with refractive aft-imaging system, the diffractive Schmidt mirror system can be used to obtain broadband performance over a specified spectral band.

5.4 Hybrid Diffractive/Reflective Aspheric Mirror

A second way to add the required aspheric terms required to correct spherical aberration introduced by a spherical mirror is to place the diffractive element directly onto the mirror surface. This has the advantage of fixing the alignment between the mirror and the corrector element. The complication is that the diffractive surface must be placed onto a curved surface.

A design for a hybrid mirror was generated and compared to the diffractive Schmidt mirror system. The design is shown in Fig. 22.

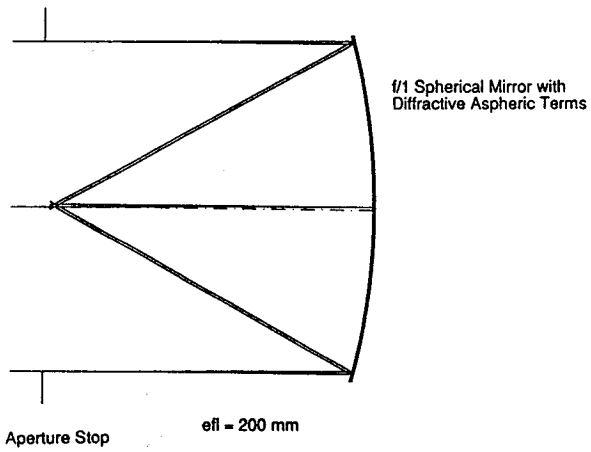

Fig. 22. Layout for a hybrid diffractive/reflective mirror. The diffractive surface is placed onto the mirrored surface.

The mirror is an f/1, 200-mm focal length mirror. A diffractive surface is used to provide aspheric terms to the wavefront to correct spherical aberration. The wavelength range is 8-12 μm. The performance of the hybrid mirror is shown in Fig. 23.

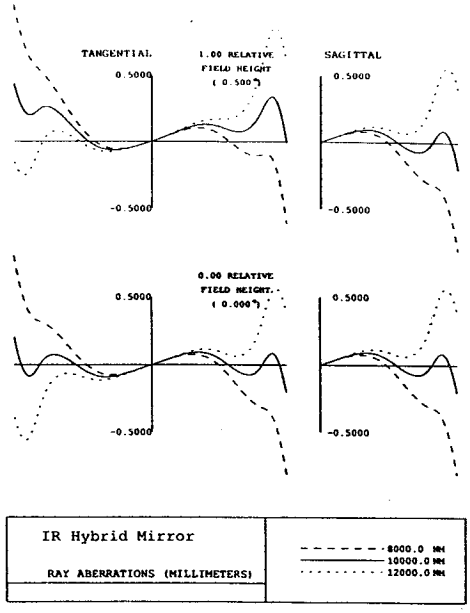

Fig. 23. Performance of the Hybrid Diffractive/Reflective Mirror. The performance is similar to the spherical mirror corrected with the diffractive Schmidt corrector plate.

The diffractive element corrects the spherical aberration but does add some chromatic aberration. Performance of the hybrid mirror is similar to the diffractive Schmidt mirror, but is much better than a similar uncorrected spherical mirror.

The minimum zone spacing for the system operating at a center wavelength of 10 μm is 680 μm. This is a very large groove spacing and easily obtainable using present fabrication technology.

6.0 Conclusions and Recommendations

Diffractive (or binary) optics technology provides optical designers with new degrees of freedom that can be used to optimize the performance and minimize the weight of optical systems. The aim of this investigation is to analyze the design of the GEO instruments that are being proposed and identify the areas where diffractive optics technology can make an impact in GEO sensor design. Several potential applications of diffractive optics technology are identified. Applications include: the use of diffractive/refractive hybrid lenses for aft-optic imagers, diffractive telescopes for narrowband imaging, sub-wavelength structured surfaces for anti-reflection and polarization control, and aberration compensation for reflective imaging systems and grating spectrometers. Applications for the GEO that have been indentified are summarized in Table IV. Preliminary optical designs for diffractive/refractive aplanatic aft-imagers, an all-diffractive telescope for LMS, and aberration correction for reflective telescopes are described.

Table IV. Diffractive Optics Applications for the GEO.

GEO Sensor	Diffractive Optics Application
Lightning Mapper Sensor (LMS)	All-diffractive telescope, anti-reflection structured (ARS) surfaces
NOAA GOES N Imager	Diffractive/refractive hybrid lenses
GeoPlatform High-resolution Interferometer Sounder (GPHIS)	Diffractive/refractive hybrid lenses
High Resolution Earth Processes Imager (HEPI)	Diffractive/refractive hybrid lenses for UV aft-imager, sub-wavelength structured (SWS) surface depolarizer
Geostationary Imager Concept Development	Diffractive Schmidt phase plate, broadband anti-reflection structured (ARS) surfaces
Solar Spectral Irradiance Monitor (SIM)	Aberration compensation for compact grating spectrometer design

Recommendations

As identified in this report, diffractive optics may provide a key technology for improving the performance and reducing the weight and cost of GEO sensors. The next phase in the development of these applications is to generate an advanced system design for specific sensor systems, identify the fabrication methods that maximize the performance of the sensor, construct a prototype system, and test the sensor's optical performance as well as a thorough environmental analysis. The applications that appear to have the biggest payoff for GEO sensor design include: diffractive/refractive hybrid lenses for aft-imagers, an all diffractive telescope for the LMS sensor, sub-wavelength structured surfaces for anti-reflection and polarization control, and aberration compensation for the compact grating spectrometers.

REPORT DOCUMENTATION PAGE

Form Approved
OMB No. 0704-0188

1. AGENCY USE ONLY (Leave blank)	2. REPORT DATE	3. REPORT TYPE AND DATES COVERED
	31 JUL 1992	Final

4. TITLE AND SUBTITLE
Diffractive Optics Technology and the NASA Geostationary Earth Observatory (GEO)

5. FUNDING NUMBERS
C H-13026D

6. AUTHOR(S)
G. Michael Morris
Robert Michaels
Dean Faklis

7. PERFORMING ORGANIZATION NAME(S) AND ADDRESS(ES)
Rochester Photonics Corporation
80 O'Connor Road
Fairport, NY 14450

8. PERFORMING ORGANIZATION REPORT NUMBER
1276-102-G-AR

9. SPONSORING/MONITORING AGENCY NAME(S) AND ADDRESS(ES)
NASA Marshall Space Flight Center
Redstone Arsenal
Huntsville, AL

10. SPONSORING/MONITORING AGENCY REPORT NUMBER

11. SUPPLEMENTARY NOTES

12a. DISTRIBUTION/AVAILABILITY STATEMENT
DOD

12b. DISTRIBUTION CODE

13. ABSTRACT *(Maximum 200 words)*

Abstract

Diffractive (or binary) optics offers unique capabilities for the development of large-aperture, high-performance, light-weight optical systems. The Geostationary Earth Observatory (GEO) will consist of a variety of instrument to monitor the environmental conditions of the earth and its atmosphere. The aim of this investigation is to analyze the design of the GEO instruments that are being proposed and identify the areas in which diffractive (or binary) optics technology can make a significant impact in GEO sensor design. Several potential applications where diffractive optics may indeed serve as a key technology for improving the performance and reducing the weight and cost of the GEO sensors have been identified. Applications include: the use of diffractive/refractive hybrid lenses for aft-optic imagers, diffractive telescopes for narrowband imaging, sub-wavelength structured surfaces for anti-reflection and polarization control, and aberration compensation for reflective imaging systems and grating spectrometers.

14. SUBJECT TERMS

15. NUMBER OF PAGES
45

16. PRICE CODE

17. SECURITY CLASSIFICATION OF REPORT	18. SECURITY CLASSIFICATION OF THIS PAGE	19. SECURITY CLASSIFICATION OF ABSTRACT	20. LIMITATION OF ABSTRACT
Unclassified	Unclassified	Unclassified	